

# The Theory of Weakly Coupled Oscillators

Michael A. Schwemmer and Timothy J. Lewis

*Department of Mathematics, One Shields Ave, University of California*

*Davis, CA 95616*

## 1 Introduction

A phase response curve (PRC) (Winfree, 1980) of an oscillating neuron measures the phase shifts in response to stimuli delivered at different times in its cycle. PRCs are often used to predict the phase-locking behavior in networks of neurons and to understand the mechanisms that underlie this behavior. There are two main techniques for doing this. Each of these techniques requires a different kind of PRC, and each is valid in a different limiting case. One approach uses PRCs to reduce neuronal dynamics to firing time maps, e.g (Ermentrout and Kopell, 1998; Guevara et al., 1986; Goel and Ermentrout, 2002; Mirollo and Strogatz, 1990; Netoff et al., 2005b; Oprisan et al., 2004). The second approach uses PRCs to obtain a set of differential equations for the phases of each neuron in the network.

For the derivation of the firing time maps, the stimuli used to generate the PRC should be similar to the input that the neuron actually receives in the network, i.e. a facsimile of a synaptic current or conductance. The firing time map technique can allow one to predict phase-locking for moderately strong coupling, but it has the limitation that the neuron must quickly return to its normal firing cycle before subsequent input arrives. Typically, this implies that input to a neuron must be sufficiently brief and that there is only a single input to a neuron each cycle. The derivation and applications of these firing time maps are discussed in Chapter ZZ.

This chapter focuses on the second technique, which is often referred to as the theory of weakly coupled oscillators (Ermentrout and Kopell, 1984; Kuramoto, 1984; Neu, 1979). The theory of weakly coupled oscillators can be used to predict phase-locking in neuronal networks with any form of coupling, but as the name suggests, the coupling between cells must be sufficiently “weak” for these predictions to be quantitatively accurate. This implies that the coupling can only have small effects on neuronal dynamics over any given period. However, these small effects can accumulate over time and lead to phase-locking in the neuronal network. The theory of weak coupling allows one to reduce the dynamics

24 of each neuron, which could be of very high dimension, to a single differential equation describing the  
25 phase of the neuron. These “phase equations” take the form of a convolution of the input to the neuron  
26 via coupling and the neuron’s infinitesimal PRC (iPRC). The iPRC measures the response to a small  
27 brief ( $\delta$ -function-like) perturbation and acts like an impulse response function or Green’s function for the  
28 oscillating neurons. Through the dimension reduction and exploiting the form of the phase equations,  
29 the theory of weakly coupled oscillators provides a way to identify phase-locked states and understand  
30 the mechanisms that underlie them.

31 The main goal of this chapter is to explain how a weakly coupled neuronal network is reduced to  
32 its phase model description. Three different ways to ‘derive’ the phase equations are presented, each  
33 providing different insight into the underlying dynamics of phase response properties and phase-locking  
34 dynamics. The first derivation (the “Seat-of-the-Pants” derivation in section 3) is the most accessible.  
35 It captures the essence of the theory of weak coupling and only requires the reader to know some  
36 basic concepts from dynamical system theory, and have a good understanding of what it means for a  
37 system to behave linearly. The second derivation (The Geometric Approach in section 4) is a little more  
38 mathematically sophisticated and provides deeper insight into the phase response dynamics of neurons.  
39 To make this second derivation more accessible, we tie all concepts back to the explanations in the  
40 first derivation. The third derivation (The Singular Perturbation Approach in section 5) is the most  
41 mathematically abstract but it provides the cleanest derivation of the phase equations. It also explicitly  
42 shows that the iPRC can be computed as a solution of the “adjoint” equations.

43 During these three explanations of the theory of weak coupling, the phase model is derived for a  
44 pair of coupled neurons to illustrate the reduction technique. The later sections (section 6 and 7) briefly  
45 discuss extensions of the phase model to include heterogeneity, noise, and large networks of neurons.

46 For more mathematically detailed discussions of the theory of weakly coupled oscillators, we direct  
47 the reader to (Ermentrout and Kopell, 1984; Hoppensteadt and Izhikevich, 1997; Kuramoto, 1984; Neu,  
48 1979).

## 49 **2 Neuronal Models and Reduction to a Phase Model**

### 50 **2.1 General Form of Neuronal Network Models**

51 The general form of a single or multi-compartmental Hodgkin-Huxley-type neuronal model (Hodgkin  
52 and Huxley, 1952) is

$$\frac{dX}{dt} = F(X), \tag{1}$$

53 where  $X$  is a  $N$ -dimensional state variable vector of containing the membrane potential(s) and gating

54 variables<sup>1</sup>, and  $F(X)$  is a vector function describing the rate of change of the variables in time. For the  
 55 Hodgkin-Huxley (HH) model (Hodgkin and Huxley, 1952),  $X = [V, m, h, n]^T$  and

$$F(X) = \begin{bmatrix} \frac{1}{C} (-g_{Na}m^3h(V - E_{Na}) - g_Kn^4(V - E_K) - g_L(V - E_L) + I) \\ \frac{m_\infty(V) - m}{\tau_m(V)} \\ \frac{h_\infty(V) - h}{\tau_h(V)} \\ \frac{n_\infty(V) - n}{\tau_n(V)} \end{bmatrix}, \quad (2)$$

56 In this chapter, we assume that the isolated model neuron (equation (1)) exhibits stable  $T$ -periodic  
 57 firing (e.g. top trace of Figure 2). In the language of dynamical systems, we assume that the model  
 58 has an asymptotically stable  $T$ -periodic *limit cycle*. These oscillations could be either due to intrinsic  
 59 conductances or induced by applied current.

60 A pair of coupled model neurons is described by

$$\frac{dX_1}{dt} = F(X_1) + \varepsilon I(X_1, X_2) \quad (3)$$

$$\frac{dX_2}{dt} = F(X_2) + \varepsilon I(X_2, X_1), \quad (4)$$

61 where  $I(X_1, X_2)$  is a vector function describing the coupling between the two neurons, and  $\varepsilon$  scales  
 62 the magnitude of the coupling term. Typically, in models of neuronal networks, cells are only coupled  
 63 through the voltage ( $V$ ) equation. For example, a pair of electrically coupled HH neurons would have  
 64 the coupling term

$$I(X_1, X_2) = \begin{bmatrix} \frac{1}{C} (g_C(V_2 - V_1)) \\ 0 \\ 0 \\ 0 \end{bmatrix}. \quad (5)$$

65 where  $g_C$  is the coupling conductance of the electrical synapse.

---

<sup>1</sup>The gating variables could be for ionic membrane conductances in the neuron, as well as those describing the output of chemical synapses.

## 2.2 Phase Models, the $G$ -Function and Phase-Locking

The power of the theory of weakly coupled oscillators is that it reduces the dynamics of each neuronal oscillator in a network to single phase equation that describes the rate of change of its relative phase,  $\phi_j$ . The phase model corresponding to the pair of coupled neurons (3-4) is of the form

$$\frac{d\phi_1}{dt} = \varepsilon H(\phi_2 - \phi_1) \quad (6)$$

$$\frac{d\phi_2}{dt} = \varepsilon H(-(\phi_2 - \phi_1)). \quad (7)$$

The following sections present three different ways of deriving the function  $H$ , which is often called the interaction function.

Subtracting the phase equation for cell 1 from that of cell 2, the dynamics can be further reduced to a single equation that governs the evolution of the phase difference between the cells,  $\phi = \phi_2 - \phi_1$

$$\frac{d\phi}{dt} = \varepsilon(H(-\phi) - H(\phi)) = \varepsilon G(\phi). \quad (8)$$

In the case of a pair of coupled Hodgkin-Huxley neurons (as described above), the number of equations in the system is reduced from the original 8 describing the dynamics of the voltage and gating variables to a single equation. The reduction method can also be readily applied to multi-compartment model neurons, e.g. (Lewis and Rinzel, 2004; Zahid and Skinner, 2009), which can render a significantly larger dimension reduction. In fact, the method has been applied to real neurons as well, e.g. (Mancilla et al., 2007).

Note that the function  $G(\phi)$  or “ $G$ -function” can be used to easily determine the phase-locking behavior of the coupled neurons. The zeros of the  $G$ -function,  $\phi^*$ , are the steady state phase differences between the two cells. For example, if  $G(0) = 0$ , this implies that the synchronous solution is a steady state of the system. To determine the stability of the steady state note that when  $G(\phi) > 0$ ,  $\phi$  will increase and when  $G(\phi) < 0$ ,  $\phi$  will decrease. Therefore, if the derivative of  $G$  is positive at a steady state ( $G'(\phi^*) > 0$ ) then the steady state is unstable. Similarly, if the derivative of  $G$  is negative at a steady state ( $G'(\phi^*) < 0$ ) then the steady state is stable. Figure 1 shows an example  $G$ -function for two coupled identical cells. Note that this system has 4 steady states corresponding to  $\phi = 0, T$  (synchrony),  $\phi = T/2$  (anti-phase), and two other non-synchronous states. It is also clearly seen that  $\phi = 0, T$  and  $\phi = T/2$  are stable steady states and the other non-synchronous states are unstable. Thus, the two cells in this system exhibit bistability, and they will either synchronize their firing or fire in anti-phase depending upon the initial conditions.

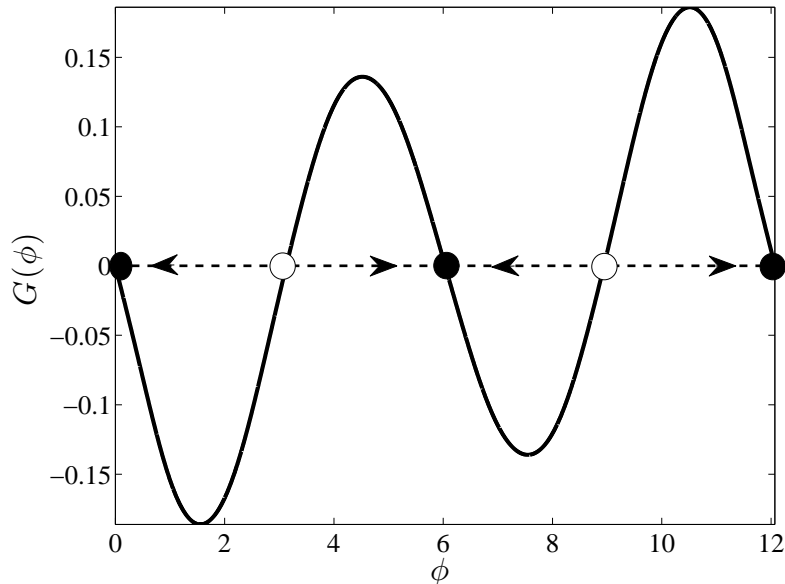


Figure 1: **Example G function.** The G function for two model Fast-Spiking (FS) interneurons (Erisir et al., 1999) coupled with gap junctions on the distal ends of their passive dendrites is plotted. The arrows show the direction of the trajectories for the system. This system has four steady state solutions  $\phi_S = 0, T$  (synchrony),  $\phi_{AP} = T/2$  (anti-phase), and two non-synchronous states. One can see that synchrony and anti-phase are stable steady-states for this system (filled in circles) while the non-synchronous solutions are unstable (open circles). Thus, depending on the initial conditions, the two neurons will fire synchronously or in anti-phase.

92 In sections 3, 4 and 5, we present three different ways of derive the interaction function  $H$  and there-  
 93 fore the  $G$ -function. These derivations make several approximations that require the coupling between  
 94 neurons to be sufficiently weak. “Sufficiently weak” implies that the neurons’ intrinsic dynamics domi-  
 95 nate the effects due to coupling at each point in the periodic cycle, i.e. during the periodic oscillations,  
 96  $|F(X_j(t))|$  should be an order of magnitude greater than  $|\varepsilon I(X_1(t), X_2(t))|$ . However, it is important to  
 97 point out that, even though the phase models quantitatively capture the dynamics of the full system for  
 98 sufficiently small  $\varepsilon$ , it is often the case that they can also capture the qualitative behavior for moderate  
 99 coupling strengths (Lewis and Rinzel, 2003; Netoff et al., 2005a).

### 100 3 A “Seat-of-the-Pants” Approach

101 This section will describe perhaps the most intuitive way of deriving the phase model for a pair of coupled  
 102 neurons (Lewis and Rinzel, 2003). The approach highlights the key aspect of the theory of weakly coupled  
 103 oscillators, which is that neurons behave linearly in response to small perturbations and therefore obey  
 104 the principle of superposition.

### 3.1 Defining Phase

$T$ -periodic firing of a model neuronal oscillator (equation (1)) corresponds to repeated circulation around an asymptotically stable  $T$ -periodic limit cycle, i.e. a closed orbit in state space  $X$ . We will denote this  $T$ -periodic limit cycle solution as  $X_{LC}(t)$ . The phase of a neuron is a measure of the time that has elapsed as the neuron's moves around its periodic orbit, starting from an arbitrary reference point in the cycle. We define the phase of the periodically firing neuron  $j$  at time  $t$  to be

$$\theta_j(t) = (t + \phi_j) \bmod T, \quad (9)$$

where  $\theta_j = 0$  is set to be at the peak of the neurons' spike (Figure 2).<sup>2</sup> The constant  $\phi_j$ , which is referred to as the *relative phase* of the  $j^{\text{th}}$  neuron, is determined by the position of the neuron on the limit cycle at time  $t = 0$ . Note that each phase of the neuron corresponds to a unique position on the cell's  $T$ -periodic limit cycle, and any solution of the uncoupled neuron model that is on the limit cycle can be expressed as

$$X_j(t) = X_{LC}(\theta_j(t)) = X_{LC}(t + \phi_j). \quad (10)$$

When a neuron is perturbed by coupling current from other neurons or by any other external stimulus, its dynamics no longer exactly adhere to the limit cycle, and the exact correspondence of time to phase (equation (9)) is no longer valid. However, when perturbations are sufficiently weak, the neuron's intrinsic dynamics are dominant. This ensures that the perturbed system remains close to the limit cycle and the inter-spike intervals are close to the intrinsic period  $T$ . Therefore, we can approximate the solution of neuron  $j$  by  $X_j(t) \simeq X_{LC}(t + \phi_j(t))$ , where the relative phase  $\phi_j$  is now a function of time  $t$ . Over each cycle of the oscillations, the weak perturbations to the neurons produce only small changes in  $\phi_j$ . These changes are negligible over a single cycle, but they can slowly accumulate over many cycles and produce substantial effects on the relative firing times of the neurons.

The goal now is to understand how the relative phase  $\phi_j(t)$  of the coupled neurons evolves slowly in time. To do this, we first consider the response of a neuron to small abrupt current pulses.

### 3.2 The Infinitesimal Phase Response Curve

Suppose that a small brief square current pulse of amplitude  $\varepsilon I_0$  and duration  $\Delta t$  is delivered to a neuron when it is at phase  $\theta^*$ . This small, brief current pulse causes the membrane potential to abruptly increase

---

<sup>2</sup>Phase is often normalized by the period  $T$  or by  $T/2\pi$ , so that  $0 \leq \theta < 1$  or  $0 \leq \theta < 2\pi$  respectively. Here, we do not normalize phase and take  $0 \leq \theta < T$ .

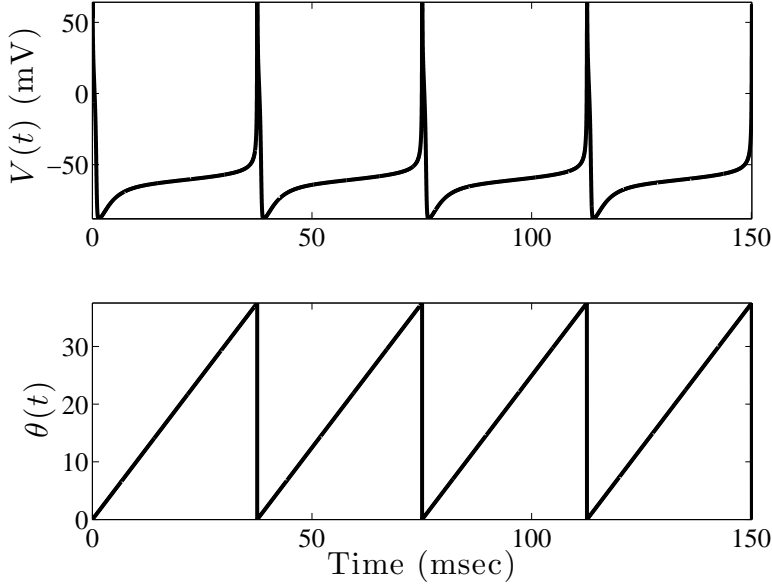


Figure 2: **Phase.** a) Voltage trace for the Fast-Spiking interneuron model from Erisir et al. (Erisir et al., 1999) with  $I_{appl} = 35 \mu A/cm^2$  showing T-periodic firing. b) The phase,  $\theta(t)$  of these oscillations increases linearly from 0 to  $T$ , and we have assumed that zero phase occurs at the peak of the voltage spike.

130 by  $\delta V \simeq \varepsilon I_0 \Delta t / C$ , i.e. the change in voltage will approximately equal the total charge delivered to the  
 131 cell by the stimulus,  $\varepsilon I_0 \Delta t$ , divided by the capacitance of the neuron,  $C$ . In general, this perturbation  
 132 can cause the cell to fire sooner (phase advance) or later (phase delay) than it would have fired without  
 133 the perturbation. The magnitude and sign of this *phase shift* depends on the amplitude and duration of  
 134 the stimulus, as well as the phase in the oscillation at which the stimulus was delivered. This relationship  
 135 is quantified by the Phase Response Curve (PRC), which gives the phase shift  $\Delta\phi$  as a function of the  
 136 phase  $\theta^*$  for a fixed  $\varepsilon I_0 \Delta t$  (Figure 3).

137 For sufficiently small and brief stimuli, the neuron will respond in a linear fashion, and the PRC will  
 138 scale linearly with the magnitude of the current stimulus

$$\Delta\phi(\theta^*) \simeq Z_V(\theta^*) \delta V = Z_V(\theta^*) \left( \frac{1}{C} \varepsilon I_0 \Delta t \right), \quad 0 \leq \theta^* < T, \quad (11)$$

139 where  $Z_V(\theta^*)$  describes the proportional phase shift as a function of the phase of the stimulus. The  
 140 function  $Z_V(\theta)$  is known as the infinitesimal phase response curve (iPRC) or the phase-dependent sen-  
 141 sitivity function for voltage perturbations. The iPRC  $Z_V(\theta)$  quantifies the normalized phase shift due  
 142 to an infinitesimally small  $\delta$ -function-like voltage-perturbation delivered at any given phase on the limit  
 143 cycle.

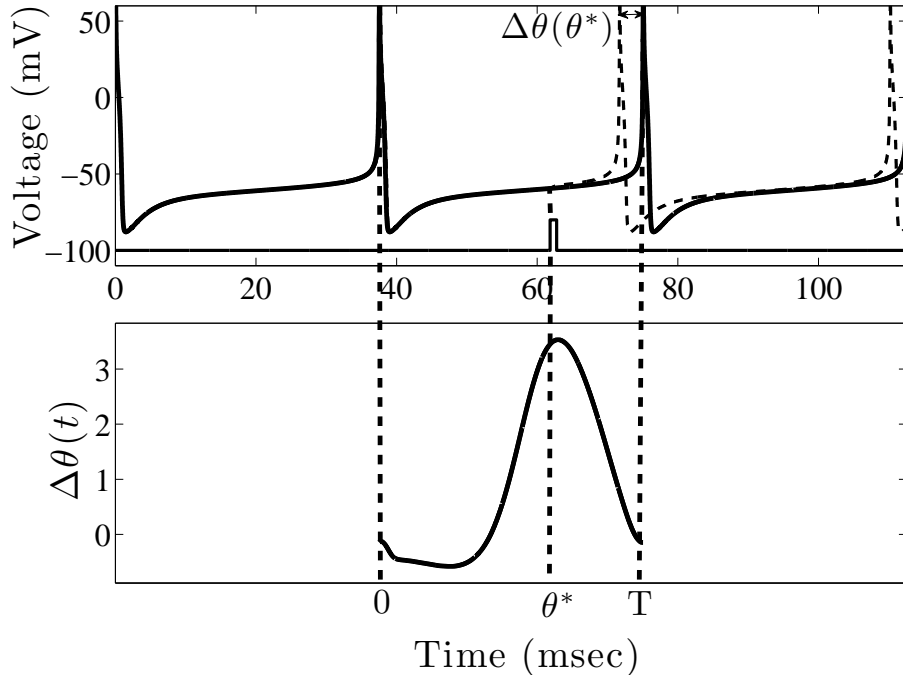


Figure 3: **Measuring the Phase Response Curve from Neurons.** The voltage trace and corresponding PRC is shown for the same FS model neuron from Figure 2. The PRC is measured from a periodically firing neuron by delivering small current pulses at every point,  $\theta^*$ , along its cycle and measuring the subsequent change in period,  $\Delta\theta$ , caused by the current pulse.

### 144 3.3 The Phase Model for a Pair of Weakly Coupled Cells

145 Now we can reconsider the pair of weakly coupled neuronal oscillators (equations (3-4)). Recall that,  
 146 because the coupling is weak, the neurons' intrinsic dynamics dominate the dynamics of the coupled-cell  
 147 system, and  $X_j(t) \simeq X_{LC}(\theta_j(t)) = X_{LC}(t + \phi_j(t))$  for  $j = 1, 2$ . This assumes that the coupling current  
 148 can only affect the speed at which cells move around their limit cycle and does not affect the amplitude  
 149 of the oscillations. Thus, the effects of the coupling are entirely captured in the slow time dynamics of  
 150 the relative phases of the cells  $\phi_j(t)$ .

151 The assumption of weak coupling also ensures that the perturbations to the neurons are sufficiently  
 152 small so that the neurons respond linearly to the coupling current. That is, (i) the small phase shifts  
 153 of the neurons due to the presence of the coupling current for a brief time  $\Delta t$  can be approximated  
 154 using the iPRC (equation (11)), and (ii) these small phase shifts in response to the coupling current sum  
 155 linearly (i.e. the principle of superposition holds). Therefore, by equation (11), the phase shift due to  
 156 the coupling current from  $t$  to  $t + \Delta t$  is

$$\begin{aligned}
\Delta\phi_j(t) &= \phi_j(t + \Delta t) - \phi_j(t) \\
&\simeq Z_V(\theta_j(t)) (\varepsilon I(X_j(t), X_k(t))) \Delta t. \\
&= Z_V(t + \phi_j(t)) (\varepsilon I(X_{LC}(t + \phi_j(t)), X_{LC}(t + \phi_k(t)))) \Delta t.
\end{aligned} \tag{12}$$

157 Furthermore, by dividing the above equation by  $\Delta t$  and taking the limit as  $\Delta t \rightarrow 0$ , we obtain a system  
158 of differential equations that govern the evolution of the relative phases of the two neurons

$$\frac{d\phi_j}{dt} = \varepsilon Z_V(t + \phi_j) I(X_{LC}(t + \phi_j), X_{LC}(t + \phi_k)), \quad j, k = 1, 2; j \neq k. \tag{13}$$

159 Note that, by integrating this system of differential equations to find the solution  $\phi_j(t)$ , we are assuming  
160 that phase shifts in response to the coupling current sum linearly.

161 The explicit time-dependence on the righthand side of equation (13) can be eliminated by “averaging”  
162 over the period  $T$ . Note that  $Z_V(t)$  and  $X_{LC}(t)$  are  $T$ -periodic functions, and the scaling of the righthand  
163 side of equation (13) by the small parameter  $\varepsilon$  indicates that changes in the relative phases  $\phi_j$  occur on  
164 a much slower time scale than  $T$ . Therefore, we can integrate the righthand side over the full period  $T$   
165 holding the values of  $\phi_j$  constant to find the average rate of change of the  $\phi_j$  over a cycle. Thus, we  
166 obtain equations that approximate the slow time evolution of the relative phases  $\phi_j$

$$\begin{aligned}
\frac{d\phi_j}{dt} &= \varepsilon \frac{1}{T} \int_0^T Z_V(\tilde{t}) (I(X_{LC}(\tilde{t}), X_{LC}(\tilde{t} + \phi_k - \phi_j))) d\tilde{t} \\
&= \varepsilon H(\phi_k - \phi_j), \quad j, k = 1, 2; j \neq k,
\end{aligned} \tag{14}$$

167 i.e. the relative phases  $\phi_j$  are assumed to be constant with respect to the integral over  $T$  in  $\tilde{t}$ , but they  
168 vary in  $t$ . This averaging process is made rigorous by averaging theory (Ermentrout and Kopell, 1991;  
169 Guckenheimer and Holmes, 1983).

170 We have reduced the dynamics of a pair of weakly coupled neuronal oscillators to an autonomous  
171 system of two differential equations describing the phases of the neurons and therefore finished the first  
172 derivation of the phase equations for a pair of weakly coupled neurons.<sup>3</sup> Note that the above derivation  
173 can be easily altered to obtain the phase model of a neuronal oscillator subjected to  $T$ -periodic external  
174 forcing as well. The crux of the derivation was identifying the iPRC and exploiting the approximately

---

<sup>3</sup>Note that this reduction is not valid when  $T$  is of the same order of magnitude as the time scale for the changes due to the weak coupling interactions (e.g. close to a SNIC bifurcation), however an alternative reduction can be performed in this case (Ermentrout, 1996).

175 linear behavior of the system in response to weak inputs. In fact, it is useful to note that the interaction  
 176 function  $H$  takes the form of a convolution of the iPRC and the coupling current, i.e. the input to the  
 177 neuron. Therefore, one can think of the iPRC as the oscillator acting like an impulse response function  
 178 or Green’s function.

### 179 3.3.1 Averaging theory

180 Averaging theory (Ermentrout and Kopell, 1991; Guckenheimer and Holmes, 1983) states that there is  
 181 a change of variables that maps solutions of

$$\frac{d\phi}{d\tilde{t}} = \varepsilon g(\phi, \tilde{t}), \quad (15)$$

182 where  $g(\phi, \tilde{t})$  is a  $T$ -periodic function in  $\phi$  and  $\tilde{t}$ , to solutions of

$$\frac{d\varphi}{dt} = \varepsilon \bar{g}(\varphi) + \mathcal{O}(\varepsilon^2), \quad (16)$$

183 where

$$\bar{g}(\varphi) = \frac{1}{T} \int_0^T g(\varphi, \tilde{t}) d\tilde{t}, \quad (17)$$

184 and  $\mathcal{O}(\varepsilon^2)$  is Landau’s “Big O” notation which represents terms that either have a scaling factor of  $\varepsilon^2$   
 185 or go to zero at the same rate as  $\varepsilon^2$  goes to zero as  $\varepsilon$  goes to zero.

## 186 4 A Geometric Approach

187 In this section, we describe a geometric approach to the theory of weakly coupled oscillators originally  
 188 introduced by Yoshiki Kuramoto (Kuramoto, 1984). The main asset of this approach is that it gives a  
 189 beautiful geometric interpretation of the iPRC and deepens our understanding of the underlying mech-  
 190 anisms of the phase response properties of neurons.

### 191 4.1 The One-to-One Map Between Points on the Limit Cycle and Phase

192 Consider again a model neuron (1) that has a stable  $T$ -periodic limit cycle solution,  $X_{LC}(t)$  such that  
 193 the neuron exhibits a  $T$ -periodic firing pattern (e.g. top trace of Figure 2). Recall that the phase of  
 194 the oscillator along its limit cycle is defined as  $\theta(t) = (t + \phi) \bmod T$ , where the relative phase  $\phi$  is a  
 195 constant that is determined by the initial conditions. Note that there is a one-to-one correspondence  
 196 between phase and each point on the limit cycle. That is, the limit cycle solution takes phase to a unique

197 point on the cycle,  $X = X_{LC}(\theta)$ , and its inverse maps each point on the limit cycle to a unique phase,  
 198  $\theta = X_{LC}^{-1}(X) = \Phi(X)$ .

199 Note that it follows immediately from the definition of phase (9) that the rate of change of phase in  
 200 time along the limit cycle is equal to 1, i.e.  $\frac{d\theta}{dt} = 1$ . Therefore, if we differentiate the map  $\Phi(X)$  with  
 201 respect to time using the chain rule for vector functions, we obtain the following useful relationship

$$\frac{d\theta}{dt} = \nabla_X \Phi(X_{LC}(t)) \cdot \frac{dX_{LC}}{dt} = \nabla_X \Phi(X_{LC}(t)) \cdot F(X_{LC}(t)) = 1, \quad (18)$$

202 where  $\nabla_X \Phi$  is the gradient of the map  $\Phi(X)$  with respect to the vector of the neuron's state variables  
 203  $X = (x_1, x_2, \dots, x_N)$

$$\nabla_X \Phi(X) = \left[ \left( \frac{\partial \Phi}{\partial x_1}, \frac{\partial \Phi}{\partial x_2}, \dots, \frac{\partial \Phi}{\partial x_N} \right) \Big|_X \right]^T. \quad (19)$$

204 (We have defined the gradient as a column vector for notational reasons).

## 205 4.2 Asymptotic Phase and the Infinitesimal Phase Response Curve

206 The map  $\theta = \Phi(X)$  is well-defined for all points  $X$  on the limit cycle. We can extend the domain of  
 207  $\Phi(X)$  to points off the limit cycle by defining the concept of *asymptotic phase*. If  $X_0$  is a point on the  
 208 limit cycle and  $Y_0$  is a point in a neighborhood of the limit cycle<sup>4</sup>, then we say that  $Y_0$  has the same  
 209 asymptotic phase as  $X_0$  if  $\|X(t; X_0) - X(t; Y_0)\| \rightarrow 0$  as  $t \rightarrow \infty$ . This means that the solution starting  
 210 at the initial point  $Y_0$  off the limit cycle converges to the solution starting at the point  $X_0$  on the limit  
 211 cycle as time goes to infinity. Therefore,  $\Phi(Y_0) = \Phi(X_0)$ . The set of all points off the limit cycle that  
 212 have the same asymptotic phase as the point  $X_0$  on the limit cycle is known as the *isochron* (Winfree,  
 213 1980) for phase  $\theta = \Phi(X_0)$ . Figure 4 shows some isochrons around the limit cycle for the Morris-Lecar  
 214 neuron (Morris and Lecar, 1981). It is important to note that the figure only plots isochrons for a few  
 215 phases and that *every* point on the limit cycle has a corresponding isochron.

216 Equipped with the concept of asymptotic phase, we can now show that the iPRC is in fact the  
 217 gradient of the phase map  $\nabla_X \Phi(X_{LC}(t))$  by considering the following phase resetting ‘‘experiment’’.  
 218 Suppose that, at time  $t$ , the neuron is on the limit cycle in state  $X(t) = X_{LC}(\theta^*)$  with corresponding  
 219 phase  $\theta^* = \Phi(X(t))$ . At this time, it receives a small abrupt external perturbation  $\varepsilon U$ , where  $\varepsilon$  is the  
 220 magnitude of the perturbation and  $U$  is the unit vector in the direction of the perturbation in state space.  
 221 Immediately after the perturbation, the neuron is in the state  $X_{LC}(\theta^*) + \varepsilon U$ , and its new asymptotic  
 222 phase is  $\tilde{\theta}^* = \Phi(X_{LC}(\theta^*) + \varepsilon U)$ . Using Taylor series,

---

<sup>4</sup>In fact, the point  $Y_0$  can be anywhere in the basin of attraction of the limit cycle.

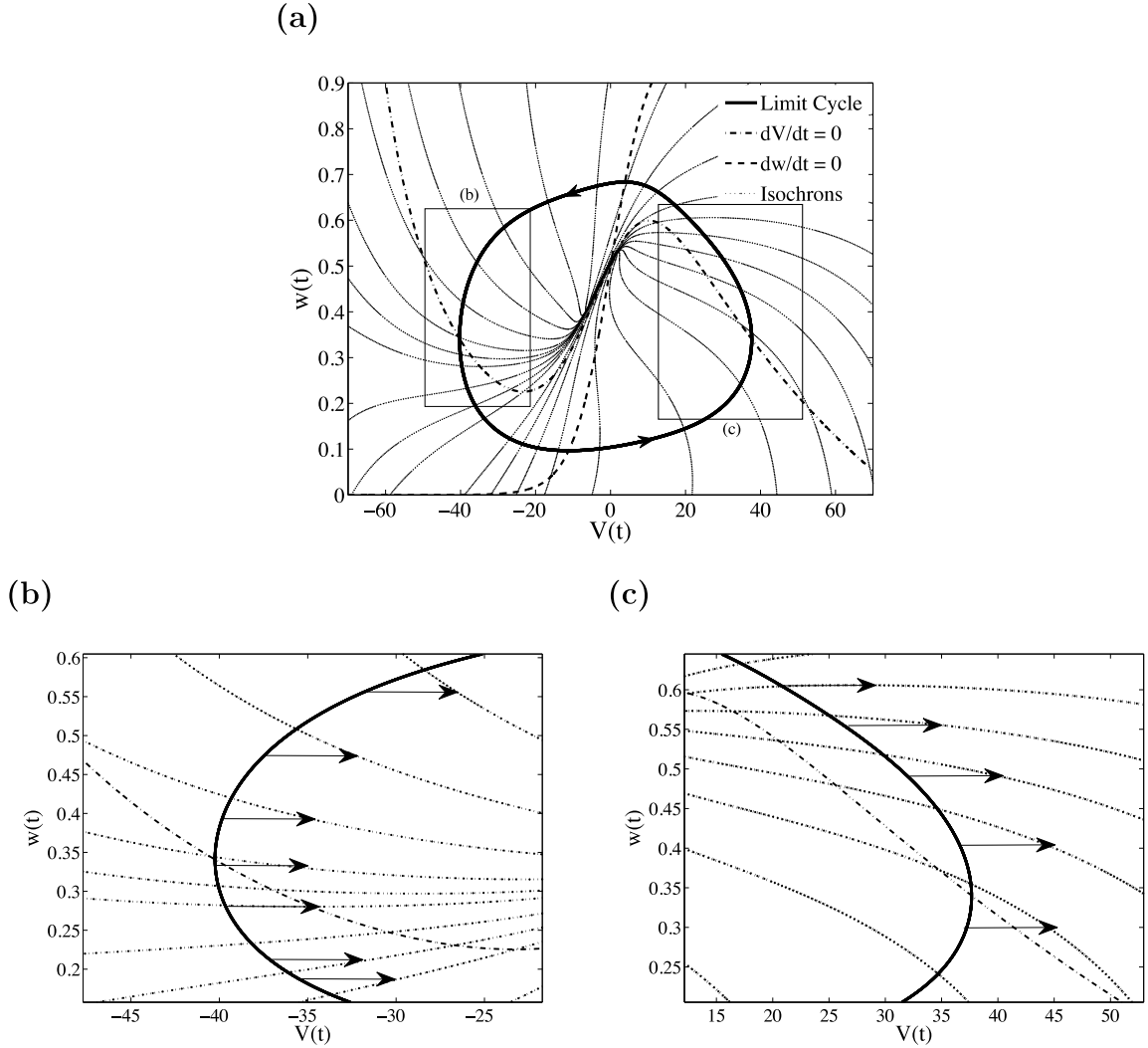


Figure 4: **Example Isochron Structure.** a) The limit cycle and isochron structure for the Morris-Lecar neuron (Morris and Lecar, 1981) is plotted along with the nullclines for the system. b) Blow up of a region on the left side of the limit cycle showing how the same strength perturbation in the voltage direction can cause different size phase delays and even a phase advance. c) Blow up of a region on the right side of the limit cycle showing also that the same size voltage perturbation can cause different size phase advances.

$$\tilde{\theta} = \Phi(X_{LC}(\theta^*) + \varepsilon U) = \Phi(X_{LC}(\theta^*)) + \nabla_X \Phi(X_{LC}(\theta^*)) \cdot (\varepsilon U) + \mathcal{O}(\varepsilon^2). \quad (20)$$

223 Keeping only the linear term (i.e.  $\mathcal{O}(\varepsilon)$  term), the phase shift of the neuron as a function of the phase  
 224  $\theta^*$  at which it received the  $\varepsilon U$  perturbation is given by

$$\Delta\phi(\theta^*) = \tilde{\theta} - \theta^* \simeq \nabla_X \Phi(X_{LC}(\theta^*)) \cdot (\varepsilon U). \quad (21)$$

225 As was done in section 3.2, we normalize the phase shift by the magnitude of the stimulus,

$$\frac{\Delta\phi(\theta^*)}{\varepsilon} \simeq \nabla_X\Phi(X_{LC}(\theta^*)) \cdot U = Z(\theta^*) \cdot U. \quad (22)$$

226 Note that  $Z(\theta) = \nabla_X\Phi(X_{LC}(\theta))$  is the iPRC. It quantifies the normalized phase shift due to a small  
 227 delta-function-like perturbation delivered at any given on the limit cycle. As was the case for the iPRC  
 228  $Z_V$  derived in the previous section (see equation (11)),  $\nabla_X\Phi(X_{LC}(\theta))$  captures only the linear response  
 229 of the neuron and is quantitatively accurate only for sufficiently small perturbations. However, unlike  $Z_V$ ,  
 230  $\nabla_X\Phi(X_{LC}(\theta))$  captures the response to perturbations in any direction in state space and not only in one  
 231 variable (e.g. the membrane potential). That is,  $\nabla_X\Phi(X_{LC}(\theta))$  is the vector iPRC; its components are  
 232 the iPRCs for every variable in the system (see Figure 5).

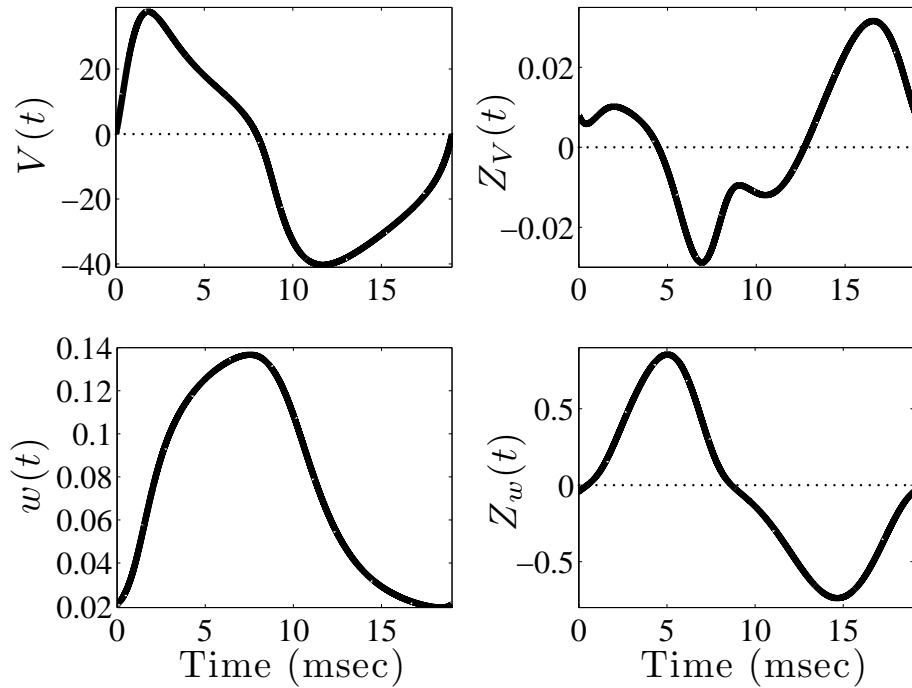


Figure 5: **iPRCs for the Morris-Lecar Neuron.** The voltage,  $V(t)$  and channel,  $w(t)$ , components of the limit cycle for the same Morris-Lecar neuron as in Figure 4 are plotted along with their corresponding iPRCs. Note that the shape of voltage iPRC can be inferred from the insets of Figure 4. For example, the isochronal structure in Figure 4 (c) reveals that perturbations in the voltage component will cause phase advances when the voltage is increasing from roughly 30 to 38 mV.

233 In the typical case of a single-compartment HH model neuron subject to an applied current pulse  
 234 (which perturbs only the membrane potential), the perturbation would be of the form  $\varepsilon U = (u, 0, 0, \dots, 0)$   
 235 where  $x_1$  is the membrane potential  $V$ . By equation (20), the phase shift is

$$\Delta\phi(\theta) = \frac{\partial\Phi}{\partial V}(X_{LC}(\theta)) u = Z_V(\theta) u, \quad (23)$$

236 which is the same as the equation (11) derived in the previous section.

237 With the understanding that  $\nabla_X\Phi(X_{LC}(t))$  is the vector iPRC, we now derive the phase model for  
238 two weakly coupled neurons.

### 239 4.3 A Pair of Weakly Coupled Oscillators

240 Now consider the system of weakly coupled neurons (3-4). We can use the map  $\Phi$  to take the variables  
241  $X_1(t)$  and  $X_2(t)$  to their corresponding asymptotic phase, i.e.  $\theta_j(t) = \Phi(X_j(t))$  for  $j = 1, 2$ . By the  
242 chain rule, we obtain the change in phase with respect to time

$$\begin{aligned} \frac{d\theta_j}{dt} &= \nabla_X\Phi(X_j(t)) \cdot \frac{dX_j}{dt} \\ &= \nabla_X\Phi(X_j(t)) \cdot [F(X_j(t)) + \varepsilon I(X_j(t), X_k(t))] \\ &= \nabla_X\Phi(X_j(t)) \cdot F(X_j(t)) + \nabla_X\Phi(X_j(t)) \cdot [\varepsilon I(X_j(t), X_k(t))] \\ &= 1 + \varepsilon \nabla_X\Phi(X_j(t)) \cdot I(X_j(t), X_k(t)), \end{aligned} \quad (24)$$

243 where we have used the “useful” relation (18). Note that the above equations are exact. However, in  
244 order to solve the equations for  $\theta_j(t)$ , we would already have to know the full solutions  $X_1(t)$  and  $X_2(t)$ ,  
245 in which case you wouldn’t need to reduce the system to a phase model. Therefore, we exploit that fact  
246 that  $\varepsilon$  is small and make the approximation  $X_j(t) \sim X_{LC}(\theta_j(t)) = X_{LC}(t + \phi_j(t))$ , i.e. the coupling is  
247 assumed to be weak enough so that it does not affect the amplitude of the limit cycle, but it can affect  
248 the rate at which the neuron moves around its limit cycle. By making this approximation in equation  
249 (24) and making the change of variables  $\theta_j(t) = t + \phi_j(t)$ , we obtain the equations for the evolution of  
250 the relative phases of the two neurons

$$\frac{d\phi_j}{dt} = \varepsilon \nabla_X\Phi(X_{LC}(t + \phi_j(t))) \cdot I(X_{LC}(t + \phi_j(t)), X_{LC}(t + \phi_k(t))). \quad (25)$$

251 Note that these equations are the vector versions of the equations (13) with the iPRC written as  
252  $\nabla_X\Phi(X_{LC}(t))$ . As described in the previous section, we can average these equations over the period  
253  $T$  to eliminate the explicit time dependence and obtain the phase model for the pair of coupled neurons

$$\frac{d\phi_j}{dt} = \varepsilon \frac{1}{T} \int_0^T \nabla_X\Phi(X_{LC}(\tilde{t})) \cdot I(X_{LC}(\tilde{t}), X_{LC}(\tilde{t} + (\phi_k - \phi_j))) d\tilde{t} = \varepsilon H(\phi_k - \phi_j). \quad (26)$$

254 Note that, while the above approach to deriving the phase equations provides substantial insight into  
 255 the geometry of the neuronal phase response dynamics, it does not provide a computational method  
 256 to compute the iPRC for model neurons, i.e. we still must directly measure the iPRC using extensive  
 257 numerical simulations as described in the previous section.

## 258 5 A Singular Perturbation Approach

259 In this section, we describe the singular perturbation approach to derive the theory of weakly coupled  
 260 oscillators. This systematic approach was developed independently by Malkin (Malkin, 1949; Malkin,  
 261 1956), Neu (Neu, 1979), and Ermentrout and Kopell (Ermentrout and Kopell, 1984). The major practical  
 262 asset of this approach is that it provides a simple method to compute iPRCs for model neurons.

263 Consider again the system of weakly coupled neurons (3-4). We assume that the isolated neurons  
 264 have asymptotically stable  $T$ -periodic limit cycle solutions  $X_{LC}(t)$  and that coupling is weak (i.e.  $\varepsilon$  is  
 265 small). As previously stated, the weak coupling has small effects on the dynamics of the neurons. On  
 266 the time-scale of a single cycle, these effects are negligible. However, the effects can slowly accumulate  
 267 on a much slower time-scale and have a substantial influence on the relative firing times of the neurons.  
 268 We can exploit the differences in these two time-scales and use the method of multiple scales to derive  
 269 the phase model.

270 First, we define a “fast time”  $t_f = t$ , which is on the time-scale of the period of the isolated neuronal  
 271 oscillator, and a “slow time”  $t_s = \varepsilon t$ , which is on the time-scale that the coupling affects the dynamics of  
 272 the neurons. Time,  $t$ , is thus a function of both the fast and slow times, i.e.  $t = f(t_f, t_s)$ . By the chain  
 273 rule,  $\frac{d}{dt} = \frac{\partial}{\partial t_f} + \varepsilon \frac{\partial}{\partial t_s}$ . We then assume that solutions  $X_1(t)$  and  $X_2(t)$  can be expressed as power-series  
 274 in  $\varepsilon$  that are dependent both on  $t_f$  and  $t_s$ ,

$$X_j(t) = X_j^0(t_f, t_s) + \varepsilon X_j^1(t_f, t_s) + \mathcal{O}(\varepsilon^2), \quad j = 1, 2.$$

275 Substituting these expansions into equations (3-4) yields

$$\begin{aligned} \frac{\partial X_j^0}{\partial t_f} + \varepsilon \frac{\partial X_j^0}{\partial t_s} + \varepsilon \frac{\partial X_j^1}{\partial t_f} + \mathcal{O}(\varepsilon^2) &= F(X_j^0 + \varepsilon X_j^1 + \mathcal{O}(\varepsilon^2)) \\ &+ \varepsilon I(X_j^0 + \varepsilon X_j^1 + \mathcal{O}(\varepsilon^2), X_k^0 + \varepsilon X_k^1 + \mathcal{O}(\varepsilon^2)), \quad j, k = 1, 2; j \neq k. \end{aligned} \quad (27)$$

276 Using Taylor series to expand the vector functions  $F$  and  $I$  in terms of  $\varepsilon$ , we obtain

$$F(X_j^0 + \varepsilon X_j^1 + \mathcal{O}(\varepsilon^2)) = F(X_j^0) + \varepsilon DF(X_j^0)X_j^1 + \mathcal{O}(\varepsilon^2) \quad (28)$$

$$\varepsilon I(X_j^0 + \varepsilon X_j^1 + \mathcal{O}(\varepsilon^2), X_k^0 + \varepsilon X_k^1 + \mathcal{O}(\varepsilon^2)) = \varepsilon I(X_j^0, X_k^0) + \mathcal{O}(\varepsilon^2), \quad (29)$$

277 where  $DF(X_j^0)$  is the Jacobian, i.e. matrix of partial derivatives, of the vector function  $F(X_j)$  evaluated  
 278 at  $X_j^0$ . We then plug these expressions into equations (27), collect like terms of  $\varepsilon$ , and equate the  
 279 coefficients of like terms.<sup>5</sup>

280 The leading order ( $\mathcal{O}(1)$ ) terms yield

$$\frac{\partial X_j^0}{\partial t_f} = F(X_j^0), \quad j = 1, 2. \quad (30)$$

281 These are the equations that describe the dynamics of the uncoupled cells. Thus, to leading order, each  
 282 cell exhibits the  $T$ -periodic limit cycle solution  $X_j^0(t_f, t_s) = X_{LC}(t_f + \phi_j(t_s))$ . Note that equation (30)  
 283 implies that the relative phase  $\phi_j$  is constant in  $t_f$ , but it can still evolve on the slow time-scale  $t_s$ .

284 Substituting the solutions for the leading order equations (and shifting  $t_f$  appropriately), the  $\mathcal{O}(\varepsilon)$   
 285 terms of equations (27) yield

$$\mathcal{L}X_j^1 \equiv \frac{\partial X_j^1}{\partial t_f} - DF(X_{LC}(t_f))X_j^1 = I(X_{LC}(t_f), X_{LC}(t_f - (\phi_j(t_s) - \phi_k(t_s)))) - X'_{LC}(t_f)\frac{d\phi_j}{dt_s}. \quad (31)$$

286 To simplify notation, we have defined the linear operator  $\mathcal{L}X \equiv \frac{\partial X}{\partial t_f} - DF(X_{LC}(t_f))X$ , which acts on a  
 287  $T$ -periodic domain and is therefore bounded. Note that equation (31) is a linear differential equation with  
 288  $T$ -periodic coefficients. In order for our power series solutions for  $X_1(t)$  and  $X_2(t)$  to exist, a solution to  
 289 equation (31) must exist. Therefore, we need to find conditions that guarantee the existence of a solution  
 290 to equation (31), i.e. conditions that ensure that the righthand side of equation (31) is in the range of  
 291 the operator  $\mathcal{L}$ . The Fredholm Alternative explicitly provides us with these conditions.

**Theorem (Fredholm's Alternative).** *Consider the following equation*

$$(*) \quad \mathcal{L}x = \frac{dx}{dt} + A(t)x = f(t); \quad x \in \mathbb{R}^N,$$

where  $A(t)$  and  $f(t)$  are continuous and  $T$ -periodic. Then, there is a continuous  $T$ -periodic solution  $x(t)$

---

<sup>5</sup>Because the equation should hold for arbitrary  $\varepsilon$ , coefficients of like terms must be equal.

to (\*) if and only if

$$(**) \quad \frac{1}{T} \int_0^T Z(t) \cdot f(t) dt = 0,$$

for each continuous  $T$ -periodic solution,  $Z(t)$ , to the adjoint problem

$$\mathcal{L}^* x = -\frac{dZ}{dt} + \{A(t)\}^T Z = 0.$$

In the language of the above theorem,

$$A(t) = -DF(X_{LC}(t_f)) \quad \text{and} \quad f(t) = I(X_{LC}(t_f), X_{LC}(t_f - (\phi_j(t_s) - \phi_k(t_s)))) - X'_{LC}(t_f) \frac{d\phi_j}{dt_s}.$$

292 Thus, the solvability condition (\*\*) requires that

$$\frac{1}{T} \int_0^T Z(t_f) \cdot \left[ I(X_{LC}(t_f), X_{LC}(t_f - (\phi_j(t_s) - \phi_k(t_s)))) - X'_{LC}(t_f) \frac{d\phi_j}{dt_s} \right] dt_f = 0 \quad (32)$$

293 where  $Z$  is a  $T$ -periodic solution of the adjoint equation

$$\mathcal{L}^* Z = -\frac{\partial Z}{\partial t_f} - DF(X_{LC}(t_f))^T Z = 0. \quad (33)$$

294 Rearranging equation (32),

$$\frac{d\phi_j}{dt_s} = \frac{1}{T} \int_0^T Z(t_f) \cdot [I(X_{LC}(t_f), X_{LC}(t_f - (\phi_j(t_s) - \phi_k(t_s))))] dt_f \quad (34)$$

295 where we have normalized  $Z(t_f)$  by

$$\frac{1}{T} \int_0^T Z(t_f) \cdot [X'_{LC}(t_f)] dt_f = \frac{1}{T} \int_0^T Z(t_f) \cdot F(X_{LC}(t_f)) dt_f = 1. \quad (35)$$

296 This normalization of  $Z(t_f)$  is equivalent to setting  $Z(0) \cdot X'_{LC}(0) = Z(0) \cdot F(X'_{LC}(0)) = 1$ , because

297  $Z(t) \cdot X'_{LC}(t)$  is a constant (see below).

298 Finally, recalling that  $t_s = \varepsilon t$  and  $t_f = t$ , we obtain the phase model for the pair of coupled neurons

$$\frac{d\phi_j}{dt} = \varepsilon \frac{1}{T} \int_0^T Z(\tilde{t}) \cdot [I(X_{LC}(\tilde{t}), X_{LC}(\tilde{t} - (\phi_j - \phi_k)))] d\tilde{t} = \varepsilon H(\phi_k - \phi_j), \quad (36)$$

299 By comparing these phase equations with those derived in the previous sections, it is clear that the

300 appropriately normalized solution to the adjoint equations  $Z(t)$  is the iPRC of the neuronal oscillator.

301 **5.0.1 A Note on the Normalization of  $Z(t)$**

$$\begin{aligned}
\frac{d}{dt} [Z(t) \cdot F(X_{LC}(t))] &= \frac{dZ}{dt} \cdot F(X_{LC}(t)) + Z(t) \cdot \frac{d}{dt} [F(X_{LC}(t))] \\
&= (-DF(X_{LC}(t))^T Z) \cdot F(X_{LC}(t)) + Z(t) \cdot (DF(X_{LC}(t))X'_{LC}(t)) \\
&= -Z(t) \cdot (DF(X_{LC}(t))F(X_{LC}(t))) + Z(t) \cdot (DF(X_{LC}(t))F(X_{LC}(t))) \\
&= 0.
\end{aligned}$$

302 This implies that  $Z(t) \cdot F(X_{LC}(t))$  is a constant. The integral form of the normalization of  $Z(t)$  (equation  
303 (35)) implies that this constant is 1. Thus,  $Z(t) \cdot F(X_{LC}(t)) = Z(t) \cdot X'_{LC}(t) = 1$  for all  $t$ , including  
304  $t = 0$ .

305 **5.1 Adjoints and Gradients**

306 The intrepid reader who has trudged their way courageously through the preceding three sections may  
307 be wondering if there is direct way to relate the gradient of the phase map  $\nabla_X \Phi(X_{LC}(t))$  to solution  
308 of the adjoint equation  $Z(t)$ . Here, we present Brown et. al's (Brown et al., 2004) direct proof that  
309  $\nabla_X \Phi(X_{LC}(t))$  satisfies the adjoint equation (33) and the normalization condition (35).

310 Consider again the system of differential equations for an isolated neuronal oscillator (1) that has  
311 an asymptotically stable  $T$ -periodic limit cycle solution  $X_{LC}(t)$ . Suppose that  $X(t) = X_{LC}(t + \phi)$  is a  
312 solution of this system that is on the limit cycle, which starts at point  $X(0) = X_{LC}(\phi)$ . Further suppose  
313 that  $Y(t) = X_{LC}(t + \phi) + p(t)$  is a solution that starts at from the initial condition  $Y(0) = X_{LC}(\phi) + p(0)$ ,  
314 where  $p(0)$  is small in magnitude. Because this initial perturbation  $p(0)$  is small and the limit cycle is  
315 stable, (i)  $p(t)$  remains small and, to  $\mathcal{O}(|p|)$ ,  $p(t)$  satisfies the linearized system

$$\frac{dp}{dt} = DF(X_{LC}(t + \phi))p, \quad (37)$$

316 and (ii) the phase difference between the two solutions is

$$\Delta\phi = \Phi(X_{LC}(t + \phi) + p(t)) - \Phi(X_{LC}(t + \phi)) = \nabla_X \Phi(X_{LC}(t + \phi)) \cdot p(t) + \mathcal{O}(|p|^2). \quad (38)$$

317 Furthermore, while the asymptotic phases of the solutions evolve in time, the phase difference between  
318 the solutions  $\Delta\phi$  remains constant. Therefore, by differentiating equation (38), we see that to  $\mathcal{O}(|p|)$

$$\begin{aligned}
0 &= \frac{d}{dt} [\nabla_X \Phi(X_{LC}(t + \phi)) \cdot p(t)] \\
&= \frac{d}{dt} [\nabla_X \Phi(X_{LC}(t + \phi))] \cdot p(t) + \nabla_X \Phi(X_{LC}(t + \phi)) \cdot \frac{dp}{dt} \\
&= \frac{d}{dt} [\nabla_X \Phi(X_{LC}(t + \phi))] \cdot p(t) + \nabla_X \Phi(X_{LC}(t + \phi)) \cdot (DF(X_{LC}(t + \phi))p(t)) \\
&= \frac{d}{dt} [\nabla_X \Phi(X_{LC}(t + \phi))] \cdot p(t) + (DF(X_{LC}(t + \phi))^T \nabla_X \Phi(X_{LC}(t + \phi))) \cdot p(t) \\
&= \left\{ \frac{d}{dt} [\nabla_X \Phi(X_{LC}(t + \phi))] + DF(X_{LC}(t + \phi))^T (\nabla_X \Phi(X_{LC}(t + \phi))) \right\} \cdot p(t).
\end{aligned}$$

319 Because  $p$  is arbitrary, the above argument implies that  $\nabla_X \Phi(X_{LC}(t))$  solves the adjoint equation (33).

320 The normalization condition simply follows from the definition of the phase map (see equation(18)), i.e.

$$\frac{d\theta}{dt} = \nabla_X \Phi(X_{LC}(t)) \cdot X'_{LC}(t) = 1. \tag{39}$$

## 321 5.2 Computing the PRC Using the Adjoint method

322 As stated in this beginning of this section, the major practical asset of the singular perturbation approach  
323 is that it provides a simple method to compute the iPRC for model neurons. Specifically, the iPRC is a  
324  $T$ -period solution to

$$\frac{dZ}{dt} = -DF(X_{LC}(t))^T Z \tag{40}$$

325 subject to the normalization constraint

$$Z(0) \cdot X'_{LC}(0) = 1. \tag{41}$$

326 This equation is the adjoint equation for the isolated model neuron (equation (1)) linearized around the  
327 limit cycle solution  $X_{LC}(t)$ .

328 In practice, the solution to equation (40) is found by integrating the equation backwards in time  
329 (Williams and Bowtell, 1997). The adjoint system has the opposite stability of the original system  
330 (equation (1)), which has an asymptotically stable  $T$ -periodic limit cycle solution. Thus, we integrate  
331 backwards in time from an arbitrary initial condition so as to dampen out the transients and arrive at  
332 the (unstable) periodic solution of equation (40). To obtain the iPRC, we normalize the periodic solution  
333 using (41). This algorithm is automated in the software package XPPAUT (Ermentrout, 2002), which is  
334 available for free on Bard Ermentrout's webpage [www.math.pitt.edu/~bard/bardware/](http://www.math.pitt.edu/~bard/bardware/).

## 6 Extensions of Phase Models for Pairs of Coupled Cells

Up to this point, we have been dealing solely with pairs of identical oscillators that are weakly coupled. In this section, we show how the phase reduction technique can be extended to incorporate weak heterogeneity and weak noise.

### 6.1 Weak Heterogeneity

Suppose that the following system

$$\frac{dX_j}{dt} = F_j(X_j) + \varepsilon I(X_k, X_j) = F(X_j) + \varepsilon [f_j(X_j) + I(X_k, X_j)] \quad (42)$$

describes two weakly coupled neuronal oscillators (note that the vector functions  $F_j(X_j)$  are now specific to the neuron). If the two neurons are weakly heterogeneous, then their underlying limit cycles are equivalent up to an  $\mathcal{O}(\varepsilon)$  difference. That is,  $F_j(X_j) = F(X_j) + \varepsilon f_j(X_j)$ , where  $f_j(X_j)$  is a vector function that captures the  $\mathcal{O}(\varepsilon)$  differences in the dynamics of cell 1 and cell 2 from the function  $F(X_j)$ . These differences may occur in various places such as the value of the neurons' leakage conductances, the applied currents, or the leakage reversal potentials, to name a few.

As in the previous sections, equation (42) can be reduced to the phase model

$$\begin{aligned} \frac{d\phi_j}{dt} &= \varepsilon \left( \frac{1}{T} \int_0^T Z(\tilde{t}) \cdot [f_j(X_{LC}(\tilde{t})) + I(X_{LC}(\tilde{t}), X_{LC}(\tilde{t} + \phi_k - \phi_j))] d\tilde{t} \right) \\ &= \varepsilon \omega_j + \varepsilon H(\phi_k - \phi_j), \end{aligned} \quad (43)$$

where  $\omega_j = \frac{1}{T} \int_0^T Z(\tilde{t}) \cdot f_j(X_{LC}(\tilde{t})) d\tilde{t}$  represents the difference in the intrinsic frequencies of the two neurons caused by the presence of the weak heterogeneity. If we now let  $\phi = \phi_2 - \phi_1$ , we obtain

$$\begin{aligned} \frac{d\phi}{dt} &= \varepsilon (H(-\phi) - H(\phi) + \Delta\omega) \\ &= \varepsilon (G(\phi) + \Delta\omega), \end{aligned} \quad (44)$$

where  $\Delta\omega = \omega_2 - \omega_1$ . The fixed points of (44) are given by  $G(\phi) = -\Delta\omega$ . The addition of the heterogeneity changes the phase-locking properties of the neurons. For example, suppose that in the absence of heterogeneity ( $\Delta\omega = 0$ ) our G function is the same as in Figure 1, in which the synchronous solution,  $\phi_S = 0$ , and the anti-phase solution,  $\phi_{AP}$ , are stable. Once heterogeneity is added, the effect will

354 be to move the neurons away from either firing in synchrony or anti-phase to a constant non-synchronous  
 355 phase shift, as in Figure 6. For example, if neuron 1 is faster than neuron 2, then  $\Delta\omega < 0$  and the stable  
 356 steady-state phase-locked values of  $\phi$  will be shifted to left of synchrony and to the left of anti-phase,  
 357 as is seen in Figure 6 when  $\Delta\omega = -0.5$ . Thus, the neurons will still be phase-locked, but in a non-  
 358 synchronous state that will either be to the left of synchronous state or to the left of the anti-phase state  
 359 depending on the initial conditions. Furthermore, if  $\Delta\omega$  is decreased further, saddle node bifurcations  
 360 occur in which a stable and unstable fixed point collide and annihilate each other.

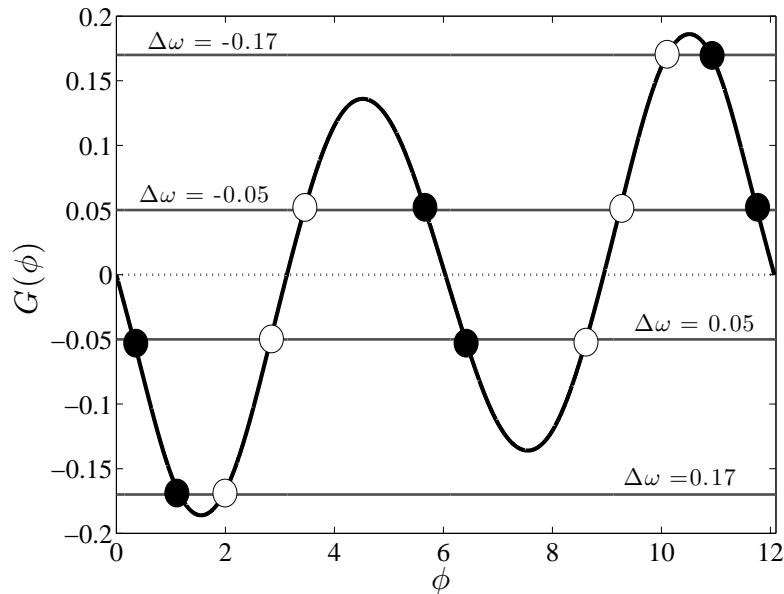


Figure 6: **Example G Function with Varying Heterogeneity.** Example of varying levels of heterogeneity with the same G function as in Figure 1. One can see that the addition of any level of heterogeneity will cause the stable steady-state phase-locked states to move to away from the synchronous and anti-phase states to non-synchronous phase-locked states. Furthermore, if the heterogeneity is large enough, the stable steady-state phase-locked states will disappear completely through saddle node bifurcations.

## 361 6.2 Weakly Coupled Neurons with Noise

362 In this section, we show how two weakly coupled neurons with additive white noise in the voltage  
 363 component can be analyzed using a probability density approach (Kuramoto, 1984; Pfeuty et al., 2005).

364 The following set of differential equations represent two weakly heterogeneous neurons being per-  
 365 turbed with additive noise

$$\frac{dX_j}{dt} = F_j(X_j) + \varepsilon I(X_k, X_j) + \delta N_j(t), \quad i, j = 1, 2; i \neq j, \quad (45)$$

366 where  $\delta$  scales the noise term to ensure that it is  $\mathcal{O}(\varepsilon)$ . The term  $N_j(t)$  is a vector with Gaussian white  
 367 noise,  $\xi_j(t)$ , with zero mean and unit variance (i.e.  $\langle \xi_j(t) \rangle = 0$  and  $\langle \xi_j(t)\xi_j(t') \rangle = \delta(t-t')$ ) in the voltage  
 368 component, and zeros in the other variable components. In this case, the system can be mapped to the  
 369 phase model

$$\frac{d\phi_j}{dt} = \varepsilon(\omega_j + H(\phi_k - \phi_j)) + \delta\sigma_\phi\xi_j(t), \quad (46)$$

370 where the term  $\sigma_\phi = \left(\frac{1}{T} \int_0^T [Z(\tilde{t})]^2 d\tilde{t}\right)^{1/2}$  comes from averaging the noisy phase equations (Kuramoto,  
 371 1984). If we now let  $\phi = \phi_2 - \phi_1$  we arrive at

$$\frac{d\phi}{dt} = \varepsilon(\Delta\omega + (H(-\phi) - H(\phi))) + \delta\sigma_\phi\sqrt{2}\eta(t), \quad (47)$$

372 where  $\Delta\omega = \omega_2 - \omega_1$  and  $\sqrt{2}\eta(t) = \xi_2(t) - \xi_1(t)$  where  $\eta(t)$  is Gaussian white noise with zero mean and  
 373 unit variance.

374 The non-linear Langevin equation (47) corresponds to the Fokker-Planck equation (Risken, 1989;  
 375 Stratonovich, 1967; Van Kampen, 1981)

$$\frac{\partial\rho}{\partial t}(\phi, t) = -\frac{\partial}{\partial\phi}[\varepsilon(\Delta\omega + G(\phi))\rho(\phi, t)] + (\delta\sigma_\phi)^2\frac{\partial^2\rho}{\partial\phi^2}(\phi, t), \quad (48)$$

376 where  $\rho(\phi, t)$  is the probability that the neurons have a phase difference of  $\phi$  at time  $t$ . The steady-state  
 377  $\left(\frac{\partial\rho}{\partial t} = 0\right)$  solution of equation (48) is

$$\rho(\phi) = \frac{1}{N}e^{M(\phi)} \left[ \frac{e^{-\alpha T\Delta\omega} - 1}{\int_0^T e^{-M(\bar{\phi})} d\bar{\phi}} \int_0^\phi e^{-M(\bar{\phi})} d\bar{\phi} + 1 \right], \quad (49)$$

378 where

$$M(\phi) = \alpha \int_0^\phi (\Delta\omega + G(\bar{\phi})) d\bar{\phi}, \quad (50)$$

379  $N$  is a normalization factor so that  $\int_0^T \rho(\phi) d\phi = 1$ , and  $\alpha = \frac{\varepsilon}{\delta^2\sigma_\phi^2}$  represents the ratio of the strength of  
 380 the coupling to the variance of the noise.

381 The steady-state distribution  $\rho(\phi)$  tells us the probability that the two neurons will have a phase  
 382 difference of  $\phi$  as time goes to infinity. Furthermore, Pfeuty et al. (Pfeuty et al., 2005) showed that  
 383 spike-train cross-correlogram of the two neurons is equivalent to the steady state distribution (49) for  
 384 small  $\varepsilon$ . Figure 7 (a) shows the cross-correlogram for two identical neurons ( $\Delta\omega = 0$ ) using the G function  
 385 from Figure 1. One can see that there is a large peak in the distribution around the synchronous solution  
 386 ( $\phi_S = 0$ ), and a smaller peak around the anti-phase solution ( $\phi_{AP} = T/2$ ). Thus, the presence of the

387 noise works to smear out the probability distribution around the stable steady-states of the noiseless  
 388 system.

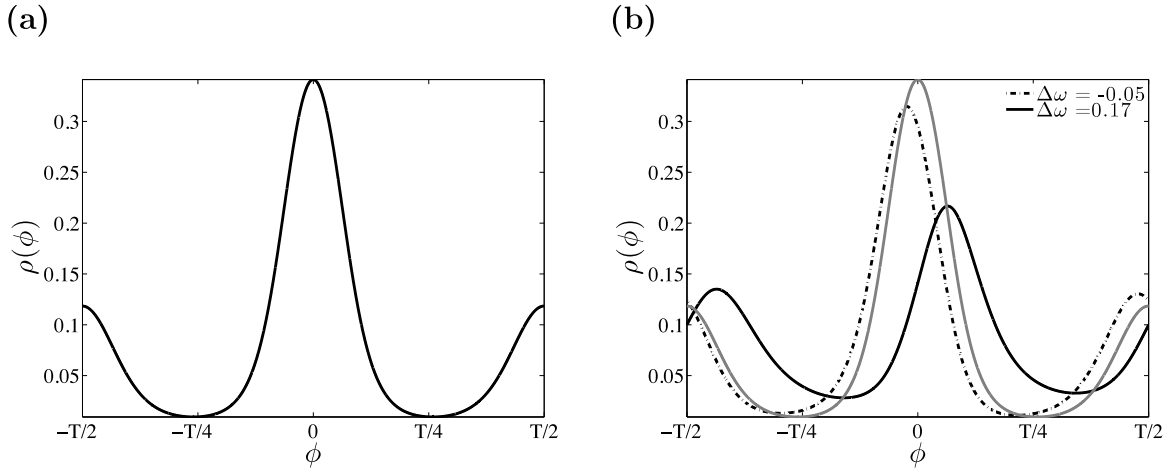


Figure 7: **The Steady-State Phase Difference Distribution  $\rho(\phi)$  is the Cross-Correlogram for the Two Neurons.** (a) Cross-correlogram for the G function given in Figure 1 with  $\alpha = 10$ . Note that we have changed the  $x$ -axis so that  $\phi$  now ranges from  $-T/2$  to  $T/2$ . The cross-correlogram has two peaks corresponding to the synchronous and anti-phase phase-locked states. This is due to the fact that in the noiseless system, synchrony and anti-phase were the only stable fixed points. (b) Cross-correlograms for two levels of heterogeneity from Figure 6. The cross-correlogram from (a) is plotted as the light solid line for comparison. The peaks in the cross-correlogram have shifted to correspond with the stable non-synchronous steady-states in Figure 6.

389 If heterogeneity is added to the G function as in Figure 6, one would expect that the peaks of the  
 390 cross-correlogram would shift accordingly so as to correspond to the stable steady-states of the noiseless  
 391 system. Figure 7 (b) shows that this is indeed the case. If  $\Delta\omega < 0$  ( $\Delta\omega > 0$ ), the stable steady-states  
 392 of the noiseless system shift to the left (right) of synchrony and to the left (right) of anti-phase, thus  
 393 causing the peaks of the cross-correlogram to shift left (right) as well. If we were to increase (decrease)  
 394 the noise, i.e. decrease (increase)  $\alpha$ , then we would see that the variance of the peaks around the stable  
 395 steady-states becomes larger (smaller), according to equation (49).

## 396 7 Networks of Weakly Coupled Neurons

397 In this section, we extend the phase model description to examine networks of weakly coupled neuronal  
 398 oscillators.

399 Suppose we have a one spatial dimension network of  $M$  weakly coupled and weakly heterogeneous  
 400 neurons

$$\frac{dX_i}{dt} = F_i(X_i) + \frac{\varepsilon}{M_0} \sum_{j=1}^M s_{ij} I(X_j, X_i), \quad i = 1, \dots, M; \quad (51)$$

401 where  $S = \{s_{ij}\}$  is the connectivity matrix of the network,  $M_0$  is the maximum number of cells that any  
 402 neuron is connected to and the factor of  $\frac{1}{M_0}$  ensures that the perturbation from the coupling is  $\mathcal{O}(\varepsilon)$ . As  
 403 before, this system can be reduced to the phase model

$$\frac{d\phi_i}{dt} = \omega_i + \frac{\varepsilon}{M_0} \sum_{j=1}^M s_{ij} H(\phi_j - \phi_i), \quad i = 1, \dots, M. \quad (52)$$

404 The connectivity matrix,  $S$ , can be utilized to examine the effects of network topology on the phase-  
 405 locking behavior of the network. For example, if we wanted to examine the activity of a network in which  
 406 each neuron is connected to every other neuron, i.e. all-to-all coupling, then

$$s_{ij} = 1, \quad i, j = 1, \dots, M. \quad (53)$$

407 Because of the non-linear nature of equation (52), analytic solutions normally cannot be found.  
 408 Furthermore, it can be quite difficult to analyze for large numbers of neurons. Fortunately, there exist  
 409 two approaches to simplifying equation (52) so that mathematical analysis can be utilized, which is not  
 410 to say that simulating the system equation (52) is not useful. Depending upon the type of interaction  
 411 function that is used, various types of interesting phase-locking behavior can be seen, such as total  
 412 synchrony, traveling oscillatory waves, or, in two spatial dimensional networks, spiral waves and target  
 413 patterns, e.g. (Ermentrout and Kleinfeld, 2001; Kuramoto, 1984).

414 A useful method of determining the level of synchrony for the network (52) is the so-called Kuramoto  
 415 synchronization index (Kuramoto, 1984)

$$r e^{2\pi i \psi / T} = \frac{1}{M} \sum_{j=1}^M e^{2\pi i \phi_j / T}, \quad (54)$$

416 where  $i = \sqrt{-1}$ ,  $\psi$  is the average phase of the network, and  $r$  is the level of synchrony of the network.  
 417 This index maps the phases,  $\phi_j$ , to vectors in the complex plane and then averages them. Thus, if the  
 418 neurons are in synchrony, the corresponding vectors will all be pointing in the same direction and  $r$  will  
 419 be equal to one. The less synchronous the network is, the smaller the value of  $r$ .

420 In the following two sections, we briefly outline two different mathematical techniques for analyzing  
 421 these phase oscillator networks in the limit as  $M$  goes to infinity.

## 7.1 Population Density Method

A powerful method to analyze large networks of all-to-all coupled phase oscillators was introduced by Strogatz and Mirollo (Strogatz and Mirollo, 1991) where they considered the so-called Kuramoto model with additive white noise

$$\frac{d\phi_i}{dt} = \omega_i + \frac{\varepsilon}{M} \sum_{j=1}^M H(\phi_j - \phi_i) + \sigma \xi(t), \quad (55)$$

where the interaction function is a simple sine function, i.e.  $H(\phi) = \sin(\phi)$ . A large body of work has been focused on analyzing the Kuramoto model as it is the simplest model for describing the onset of synchronization in populations of coupled oscillators (Acebrón et al., 2005; Strogatz, 2000). However, in this section, we will examine the case where  $H(\phi)$  is a general  $T$ -periodic function.

The idea behind the approach of (Strogatz and Mirollo, 1991) is to derive the Fokker-Planck equation for (55) in the limit as  $M \rightarrow \infty$ , i.e. the number of neurons in the network is infinite. As a first step, note that by equating real and imaginary parts in equation (54) we arrive at the following useful relations

$$r \cos(2\pi(\psi - \phi_i)/T) = \frac{1}{M} \sum_{j=1}^M \cos(2\pi(\phi_j - \phi_i)/T) \quad (56)$$

$$r \sin(2\pi(\psi - \phi_i)/T) = \frac{1}{M} \sum_{j=1}^M \sin(2\pi(\phi_j - \phi_i)/T). \quad (57)$$

Next, we note that since  $H(\phi)$  is  $T$ -periodic, we can represent it as a Fourier series

$$H(\phi_j - \phi_i) = \frac{1}{T} \sum_{n=0}^{\infty} a_n \cos(2\pi n(\phi_j - \phi_i)/T) + b_n \sin(2\pi n(\phi_j - \phi_i)/T). \quad (58)$$

Recognizing that equations (56) and (57) are averages of the functions cosine and sine, respectively, over the phases of the other oscillators, we see that, in the limit as  $M$  goes to infinity (Neltner et al., 2000; Strogatz and Mirollo, 1991)

$$r a_n \cos(2\pi n(\psi_n - \phi)/T) = a_n \int_{-\infty}^{\infty} \int_0^T g(\omega) \rho(\tilde{\phi}, \omega, t) \cos(2\pi n(\tilde{\phi} - \phi)/T) d\tilde{\phi} d\omega \quad (59)$$

$$r b_n \sin(2\pi n(\psi_n - \phi)/T) = b_n \int_{-\infty}^{\infty} \int_0^T g(\omega) \rho(\tilde{\phi}, \omega, t) \sin(2\pi n(\tilde{\phi} - \phi)/T) d\tilde{\phi} d\omega, \quad (60)$$

where we have used the Fourier coefficients of  $H(\phi_j - \phi_i)$ .  $\rho(\phi, \omega, t)$  is the density of oscillators with uncoupled frequency  $\omega$  and phase  $\phi$  at time  $t$ , and  $g(\omega)$  is the density function for the distribution of the

439 frequencies of the oscillators. Furthermore,  $g(\omega)$  also satisfies  $\int_{-\infty}^{\infty} g(\omega)d\omega = 1$ . With all this in mind,  
 440 we can now rewrite the infinite  $M$  approximation of equation (55)

$$\frac{d\phi}{dt} = \omega + \varepsilon \frac{1}{2\pi} \sum_{n=0}^{\infty} [ra_n \cos(2\pi n(\psi_n - \phi)/T) + rb_n \sin(2\pi n(\psi_n - \phi)/T)] + \sigma\xi(t). \quad (61)$$

441 The above nonlinear Langevin equation corresponds to the Fokker-Planck equation

$$\frac{\partial \rho}{\partial t}(\phi, \omega, t) = -\frac{\partial}{\partial \phi} [J(\phi, t)\rho(\phi, \omega, t)] + \frac{\sigma^2}{2} \frac{\partial^2 \rho}{\partial \phi^2}(\phi, \omega, t), \quad (62)$$

442 with

$$J(\phi, t) = \omega + \varepsilon \frac{1}{T} \sum_{n=0}^{\infty} [ra_n \cos(2\pi n(\psi_n - \phi)/T) + rb_n \sin(2\pi n(\psi_n - \phi)/T)], \quad (63)$$

443 and  $\int_0^T \rho(\phi, \omega, t)d\phi = 1$  and  $\rho(\phi, \omega, t) = \rho(\phi + T, \omega, t)$ . Equation (62) tells us how the fraction of  
 444 oscillators with phase  $\phi$  and frequency  $\omega$  evolves with time. Note that equation (62) has the trivial  
 445 solution  $\rho_0(\phi, \omega, t) = \frac{1}{T}$ , which corresponds to the incoherent state in which the phases of the neurons  
 446 are uniformly distributed between 0 and  $T$ .

447 To study the onset of synchronization in these networks, Strogatz and Mirollo (Strogatz and Mirollo,  
 448 1991) and others, e.g. (Neltner et al., 2000), linearized equation (62) around the incoherent state,  $\rho_0$ , in  
 449 order to determine its stability. They were able to prove that below a certain value of  $\varepsilon$ , the incoherent  
 450 state is neutrally stable and then loses stability at some critical value  $\varepsilon = \varepsilon_C$ . After this point, the  
 451 network becomes more and more synchronous as  $\varepsilon$  is increased.

## 452 7.2 Continuum Limit

453 Although the population density approach is powerful method for analyzing the phase-locking dynamics  
 454 of neuronal networks, it is limited by the fact that it does not take into account spatial effects of neuronal  
 455 networks. An alternative approach to analyzing (52) in the large  $M$  limit that takes into account spatial  
 456 effects is to assume that the network of neuronal oscillators forms a spatial continuum (Bressloff and  
 457 Coombes, 1997; Crook et al., 1997; Ermentrout, 1985).

458 Suppose that we have a one-dimensional array of neurons in which the  $j^{th}$  neuron occupies the  
 459 position  $x_j = j\Delta x$  where  $\Delta x$  is the spacing between the neurons. Further suppose that the connectivity  
 460 matrix is defined by  $S = \{s_{ij}\} = W(|x_j - x_i|)$ , where  $W(|x|) \rightarrow 0$  as  $|x| \rightarrow \infty$  and  $\sum_{j=-\infty}^{\infty} W(x_j)\Delta x = 1$   
 461 For example, the spatial connectivity matrix could correspond to a Gaussian function,  $W(|x_j - x_i|) =$   
 462  $e^{-\frac{|x_j - x_i|^2}{2\sigma^2}}$ , so that closer neurons have more strongly coupled to each other than to neurons that are

463 further apart. We can now rewrite equation (52) as

$$\frac{d\phi}{dt}(x_i, t) = \omega(x_i) + \varepsilon \sum_{j=-\infty}^{\infty} [W(|x_j - x_i|) \Delta x H(\phi(x_j, t) - \phi(x_i, t))], \quad (64)$$

464 where  $\phi(x_i, t) = \phi_i(t)$ ,  $\omega(x_i) = \omega_i$  and we have taken  $1/M = \Delta x$ . By taking the limit of  $\Delta x \rightarrow 0$   
 465 ( $M \rightarrow \infty$ ) in equation (64), we arrive at the continuum phase model

$$\frac{\partial\phi}{\partial t}(x, t) = \omega(x) + \varepsilon \int_{-\infty}^{\infty} W(|x - \bar{x}|) H(\phi(\bar{x}, t) - \phi(x, t)) d\bar{x}, \quad (65)$$

466 where  $\phi(x, t)$  is the phase of the oscillator at position  $x$  and time  $t$ . Note that this continuum phase  
 467 model can be modified to account for finite spatial domains (Ermentrout, 1992) and to include multiple  
 468 spatial dimensions.

469 Various authors have utilized this continuum approach to prove results about the stability of the  
 470 synchrony and traveling wave solutions of equation (65) (Bressloff and Coombes, 1997; Crook et al.,  
 471 1997; Ermentrout, 1985; Ermentrout, 1992). For example, Crook et al. (Crook et al., 1997) were able  
 472 to prove that presence of axonal delay in synaptic transmission between neurons can cause the onset  
 473 of traveling wave solutions. This is due to the presence of axonal delay which encourages larger phase  
 474 shifts between neurons that are further apart in space. Similarly, Bressloff and Coombes (Bressloff and  
 475 Coombes, 1997) derived the continuum phase model for a network of integrate-and-fire neurons coupled  
 476 with excitatory synapses on their passive dendrites. Using this model, they were able to show that long  
 477 range excitatory coupling can cause the system to undergo a bifurcation from the synchronous state to  
 478 traveling oscillatory waves. For a rigorous mathematical treatment of the existence and stability results  
 479 for general continuum and discrete phase model neuronal networks, we direct the reader to (Ermentrout,  
 480 1992).

## 481 8 Summary

- 482 • The infinitesimal PRC (iPRC) of a neuron measures its sensitivity to infinitesimally small pertur-  
 483 bations at every point along its cycle.
- 484 • The theory of weak coupling utilizes the iPRC to reduce the complexity of neuronal network to  
 485 consideration of a single phase variable for every neuron.
- 486 • The theory is valid only when the perturbations to the neuron, from coupling or an external  
 487 source, is sufficiently “weak” so that the neuron’s intrinsic dynamics dominate the influence of the

488 coupling. This implies that coupling does not cause the neuron's firing period to differ greatly from  
489 its unperturbed cycle.

- 490 • For two weakly coupled neurons, the theory allows one to reduce the dynamics to consideration of  
491 a single equation describing how the phase difference of the two oscillators changes in time. This  
492 allows for the prediction of the phase-locking behavior of the cell-pair through simple analysis of  
493 the phase difference equation.
- 494 • The theory of weak coupling can be extended to incorporate effects from weak heterogeneity and  
495 weak noise.

496 *Acknowledgements.* This work was supported by the National Science Foundation under grants DMS-  
497 09211039 and DMS-0518022.

## 498 References

- 499 Acebrón, J., Bonilla, L., Vicénte, C., Ritort, F., and Spigler, R. (2005). The kuramoto model: A simple  
500 paradigm for synchronization phenomena. *Rev. Mod. Phys.*, 77:137–185.
- 501 Bressloff, P. and Coombes, S. (1997). Synchrony in an array of integrate-and-fire neurons with dendritic  
502 structure. *Phys. Rev. Lett.*, 78:4665–4668.
- 503 Brown, E., Moehlis, J., and Holmes, P. (2004). On the phase reduction and response dynamics of neural  
504 oscillator populations. *Neural Comp.*, 16:673–715.
- 505 Crook, S., Ermentrout, G., Vanier, M., and Bower, J. (1997). The role of axonal delay in the synchro-  
506 nization of networks of coupled cortical oscillators. *J. Comp. Neurosci.*, 4:161–172.
- 507 Erisir, A., Lau, D., Rudy, B., and Leonard, C. (1999). Function of specific  $k^+$  channels in sustained  
508 high-frequency firing of fast-spiking neocortical interneurons. *J. Neurophysiol.*, 82:2476–2489.
- 509 Ermentrout, B. (2002). *Simulating, Analyzing, and Animating Dynamical Systems: A Guide to XPPAUT*  
510 *for Researchers and Students*. SIAM.
- 511 Ermentrout, G. (1985). The behavior of rings of coupled oscillators. *J. Math. Biology*, 23:55–74.
- 512 Ermentrout, G. (1992). Stable periodic solutions to discrete and continuum arrays of weakly coupled  
513 nonlinear oscillators. *SIAM J. Appl. Math.*, 52(6):1665–1687.

- 514 Ermentrout, G. (1996). Type 1 membranes, phase resetting curves, and synchrony. *Neural Computation*,  
515 8:1979–1001.
- 516 Ermentrout, G. and Kleinfeld, D. (2001). Traveling electrical waves in cortex: Insights from phase  
517 dynamics and speculation on a computational role. *Neuron*, 29:33–44.
- 518 Ermentrout, G. and Kopell, N. (1984). Frequency plateaus in a chain of weakly coupled oscillators, i.  
519 *SIAM J. Math. Anal.*, 15(2):215–237.
- 520 Ermentrout, G. and Kopell, N. (1991). Multiple pulse interactions and averaging in systems of coupled  
521 neural oscillators. *J. Math. Bio.*, 29:33–44.
- 522 Ermentrout, G. and Kopell, N. (1998). Fine structure of neural spiking and synchronization in the  
523 presence of conduction delays. *Proc. Nat. Acad. of Sci.*, 95(3):1259–1264.
- 524 Goel, P. and Ermentrout, G. (2002). Synchrony, stability, and firing patterns in pulse-coupled oscillators.  
525 *Physica D*, 163:191–216.
- 526 Guckenheimer, J. and Holmes, P. (1983). *Nonlinear Oscillations, Dynamical Systems, and Bifurcations*  
527 *of Vector Fields*. Springer-Verlag, NY.
- 528 Guevara, M. R., Shrier, A., and Glass, L. (1986). Phase resetting of spontaneously beating embryonic  
529 ventricular heart cell aggregates. *Am J Physiol Heart Circ Physiol*, 251(6):H1298–1305.
- 530 Hodgkin, A. and Huxley, A. (1952). A quantitative description of membrane current and its application  
531 to conduction and excitation in nerve. *J. Physiol.*, 117:500–544.
- 532 Hoppensteadt, F. C. and Izhikevich, E. M. (1997). *Weakly Connected Neural Networks*. Springer-Verlag,  
533 New York.
- 534 Kuramoto, Y. (1984). *Chemical Oscillations, Waves, and Turbulence*. Springer-Verlag, Berlin.
- 535 Lewis, T. and Rinzel, J. (2003). Dynamics of spiking neurons connected by both inhibitory and electrical  
536 coupling. *J. Comp. Neurosci.*, 14:283–309.
- 537 Lewis, T. and Rinzel, J. (2004). Dendritic effects in networks of electrically coupled fast-spiking interneu-  
538 rons. *Neurocomputing*, 58-60:145–150.
- 539 Malkin, I. (1949). *Methods of Poincare and Liapunov in Theory of Non-Linear Oscillations*. Gostexizdat,  
540 Moscow.
- 541 Malkin, I. (1956). *Some Problems in Nonlinear Oscillation Theory*. Gostexizdat, Moscow.

- 542 Mancilla, J., Lewis, T., Pinto, D., Rinzel, J., and Connors, B. (2007). Synchronization of electrically  
543 coupled pairs of inhibitory interneurons in neocortex. *J. Neurosci.*, 27(8):2058–2073.
- 544 Mirollo, R. and Strogatz, S. (1990). Synchronization of pulse-coupled biological oscillators. *SIAM J.*  
545 *Applied Math.*, 50(6):1645–1662.
- 546 Morris, C. and Lecar, H. (1981). Voltage oscillations in the barnacle giant muscle fiber. *Biophys J*,  
547 35:193–213.
- 548 Neltner, L., Hansel, D., Mato, G., and Meunier, C. (2000). Synchrony in heterogeneous networks of  
549 spiking neurons. *Neural Comp.*, 12:1607–1641.
- 550 Netoff, T., Acker, C., Bettencourt, J., and White, J. (2005a). Beyond two-cell networks: experimental  
551 measurement of neuronal responses to multiple synaptic inputs. *J. Comput. Neurosci.*, 18:287–295.
- 552 Netoff, T., Banks, M., Dorval, A., Acker, C., Haas, J., Kopell, N., and White, J. (2005b). Synchronization  
553 of hybrid neuronal networks of the hippocampal formation strongly coupled. *J. Neurophysiol.*,  
554 93:1197–1208.
- 555 Neu, J. (1979). Coupled chemical oscillators. *SIAM J. Appl. Math.*, 37(2):307–315.
- 556 Oprisan, S., Prinz, A., and Canavier, C. (2004). Phase resetting and phase locking in hybrid circuits of  
557 one model and one biological neuron. *Biophys. J.*, 87:2283–2298.
- 558 Pfeuty, B., Mato, G., Golomb, D., and Hansel, D. (2005). The combined effects of inhibitory and electrical  
559 synapses in synchrony. *Neural Computation*, 17:633–670.
- 560 Risken, H. (1989). *The Fokker-Planck Equation: Methods of Solution and Applications*. Springer-Verlag,  
561 NY.
- 562 Stratonovich, R. (1967). *Topics in the Theory of Random Noise*. Gordon and Breach, NY.
- 563 Strogatz, S. (2000). From kuramoto to crawford: Exploring the onset of synchronization in populations  
564 of coupled oscillators. *Physica D*, 143:1–20.
- 565 Strogatz, S. and Mirollo, R. (1991). Stability of incoherence in a population of coupled oscillators. *J.*  
566 *Stat. Physics*, 63:613–635.
- 567 Van Kampen, N. (1981). *Stochastic Processes in Physics and Chemistry*. Amsterdam: Elsevier Science.
- 568 Williams, T. and Bowtell, G. (1997). The calculation of frequency-shift functions for chains of coupled  
569 oscillators, with application to a network model of the lamprey locomotor pattern generator. *J.*  
570 *Comput. Neurosci.*, 4:47–55.

571 Winfree, A. T. (1980). *The Geometry of Biological Time*. Springer, NY.

572 Zahid, T. and Skinner, F. (2009). Predicting synchronous and asynchronous network groupings of hip-  
573 pocampal interneurons coupled with dendritic gap junctions. *Brain Research*, 1262:115 – 129.